Title	Fabrication and Characterization of Cross-linked Organic Thin Films with Nonlinear Mass Densities
Author(s)	Rashed, Md. A; Laokroekkiat, Salinthip; Hara, Mitsuo; Nagano, Shusaku; Nagao, Yuki
Citation	Langmuir, 32(23): 5917-5924
Issue Date	2016-05-13
Type	Journal Article
Text version	author
URL	http://hdl.handle.net/10119/14268
Rights	Md. A. Rashed, Salinthip Laokroekkiat, Mitsuo Hara, Shusaku Nagano and Yuki Nagao, Langmuir, 2016, 32(23), pp.5917-5924. This document is the unedited author's version of a Submitted Work that was subsequently accepted for publication in Langmuir, copyright (c) American Chemical Society after peer review. To access the final edited and published work, see http://dx.doi.org/10.1021/acs.langmuir.6b00540
Description	

Fabrication and Characterization of Cross-linked Organic Thin Films with Nonlinear Mass Densities

Md. A. Rashed,[†] Salinthip Laokroekkiat,[†] Mitsuo Hara,[‡]

Shusaku Nagano,[§] Yuki Nagao[†*]

[†]*School of Materials Science, Japan Advanced Institute of Science and Technology, 1-1 Asahidai, Nomi, Ishikawa 923-1292, Japan*

[‡]*Department of Molecular Design & Engineering, Graduate School of Engineering, Nagoya University, Furo-cho, Chikusa, Nagoya 464-8603, Japan*

[§]*Nagoya University Venture Business Laboratory, Nagoya University, Furo-cho, Chikusa, Nagoya 464-8603, Japan*

ABSTRACT

Urea (bonded) cross-linked multilayer thin film by sequential deposition of bifunctional and tetrafunctional molecular building blocks was demonstrated. Multilayer growth as a function of deposition cycles was inspected using UV-vis absorption spectroscopy. From IR results, three characteristic infrared bands of amide I, amide II, and asymmetric ν_a(N-C-N) stretching band confirmed the formation of polyurea networks by alternate dipping into solutions of amine and isocyanate functionalities monomers. The deconvoluted component from the C 1s and N 1s spectra from X-ray photoelectron spectroscopy (XPS) shows clear evidence of stable polyurea networks. Enhancement of structural periodicity with film growth was demonstrated by grazing incidence small

1

angle X-ray scattering (GI-SAXS) measurements. The thin film near the substrate surface seems to have an amorphous structure. However, molecular ordering improves in the surface normal direction of the substrate with a certain number of deposited layers. Constant mass density was not observed with deposition cycles. The mass density increased upto 16% within deposited layers from proximate layers to those extending away from the substrate surface. This difference in packing density might derive from the different degrees of cross-linking among layers proximate to the substrate surface and extending away from the surface.

Keywords: molecular layer deposition, covalent bond, multilayer films, polyurea, layer-by-layer

1. INTRODUCTION

Cross-linked organic thin films have garnered much attention recently for their higher density,[1] better mechanical strength,[2] and chemical stability.[3,4] Demand for cross-linked nanoscale organic thin films has increased rapidly for conventional applications such as organic thin film transistors[5,6], purification membranes etc.[7] However, the synthesis of thin films with sub-nanometer scale is still challenging. For the synthesis of organic thin films, spin-coating[8] and Langmuir–Blodgett (LB)[9] are well-known and useful techniques. Another simple and versatile technique to prepare multilayer organic thin

films is molecular layer deposition (MLD)[10–12], which uses a layer-by-layer (LbL)[13,14] fashion to prepare multilayer thin films with sub-nanometer scale. To date, most MLD processes have been conducted with polymerization reaction of volatile bifunctional monomers under vacuum condition. Polymeric thin films have been reported such as polyamides,[15–17] polyimides,[18–22] polyurethane,[23] polyureas,[1, 24–27] polythiourea,[28] and polyester.[29] However, this vapor-based MLD technique is inapplicable for monomers with high molar mass and low vapor pressure.[30] Because of the high boiling point of monomers, excess adsorbed monomers onto the substrate surface by vapor deposition cannot be removed completely, which hinders single molecular layer deposition. Moreover, with vacuum-based reaction system, it is difficult to use a catalyst or pH change in the reaction media to make a non-spontaneous reaction a spontaneous one.[26] Solution-based MLD offers an exclusive route to overcoming these problems. Stafford and co-workers reported multilayer cross-linked polyamide thin film using solution-based molecular layer-by-layer (mLbL) synthesis. They used bifunctional m-phenylene diamine and trifunctional trimesoyl chloride monomers to fabricate organic multilayer thin films.[31,32] Recent reports by Qian *et al.* and Kim *et al.* show cross-linked polyamide and polyurea thin films by polymerization of the same symmetrical tetrafunctional monomers to produce three-dimensional (3D) covalent

bonded molecular networks via LbL dipping technique.[30, 33]

Our approach to fabrication of 3D covalent bonded multilayer thin films is based on sequential deposition of different symmetrical monomers, such as bifunctional 1,3-phenylene diisocyanate (PDI) and tetrafunctional tetrakis(4-aminophenyl)methane (TAPM), on a 3-aminopropyltrimethoxysilane (APTMS) modified amine terminated surface. The longer urea chains with combinations of different symmetrical monomers lead to different cross-linking states within multilayer growth. This different degree of cross-linking might be facilitated by changing the molecule–molecule interaction proximate to the substrate surface and extending away from the substrate surface. It is reasonable to consider that intermolecular interaction apart from the substrate surface is considerably higher than the intermolecular interactions among monomers near the surface. It is also rational to infer that molecular networks extending away from the substrate surface exhibit higher cross-linking than molecular networks located near the substrate surface. Presumably, this different degree of cross-linking provides films with variable densities among layers (with a certain thickness) proximate to the substrate surface and extending away from the substrate surface (Figure 1).
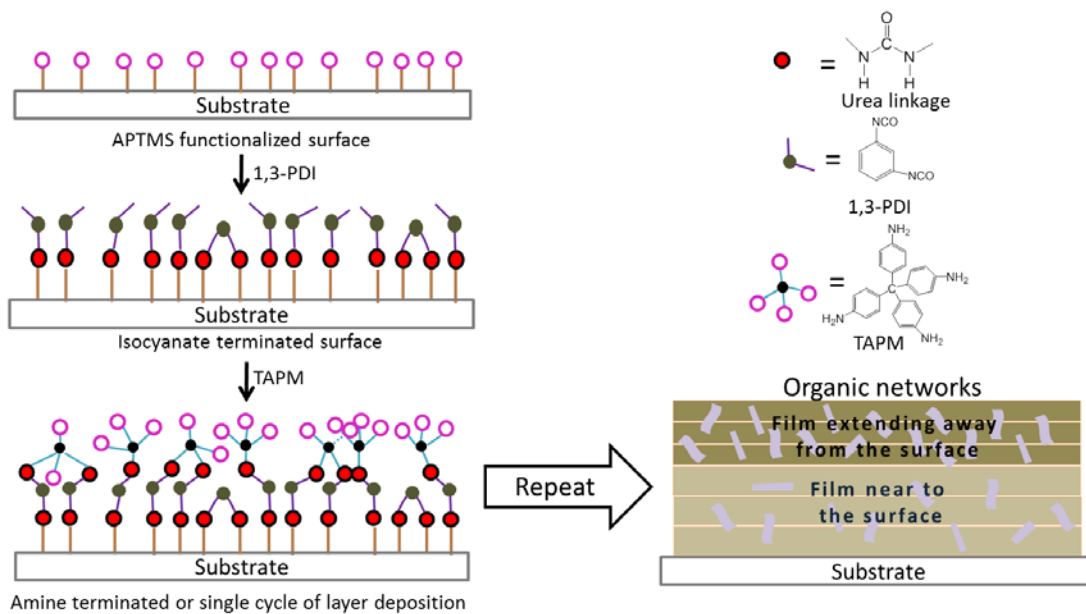
Figure 1. Schematic illustration of molecular layer deposition (MLD) process on a solid surface and the chemical structure of 1,3-PDI and TAPM monomers.

This work shows the synthesis and characterization of a new class of cross-linked multilayer polyurea thin films using 3D covalent bonded molecular networks with nonlinear mass densities via solution-based MLD technique. Infrared spectroscopy (IR) and X-ray photoelectron spectroscopy (XPS) confirmed the urea bond formation between the reaction of amine and isocyanate functionalities. UV-vis absorption spectroscopy demonstrated multilayer growth. The thickness of multilayer polyurea films on the silicon substrate was measured using atomic force microscopy (AFM) and X-ray reflective (XRR) techniques. The mass density and degree of molecular ordering with film growth were examined, respectively, using X-ray reflectivity (XRR) analysis

5

and grazing incidence small angle X-ray scattering (GI-SAXS) measurements.

2. EXPERIMENTAL

2.1. Materials

As molecular building blocks, tetrakis(4-aminophenyl)methane (TAPM) and 1,3-phenylene diisocyanate (PDI) were purchased, respectively, from Aldrich Chemical Co. Inc., USA and Tokyo Chemical Industry Co. Ltd., Japan. Using recrystallization technique, 98% pure commercial PDI was purified further. 3-Aminopropyltrimethoxysilane (APTMS, >96%) was purchased from Tokyo Chemical Industry Co. Ltd., Japan, and was used as received. All solvents were purchased as super-dehydrated and AR grade from Wako Pure Chemical Industries Ltd., Japan and were used without further purification.

2.2. Fabrication of Multilayer Thin Films on Solid Surface

Multilayer thin films were synthesized onto quartz substrates (25×15 mm^2, $t = 0.5$ mm) and silicon wafers (30×20 mm^2, $t = 0.525$ mm). Prior to multilayer formation, substrates were cleaned using 2-propanol with sonication (three times each, 15 min duration), and were then dried and kept in the clean bench. The cleaned substrates were immersed into 10 mM amine functionalized 3-aminopropyltrimethoxysilane (APTMS) in ethanol solution at room temperature for 1 hr under Ar atmosphere with constant

stirring. After taking out from the APTMS solution, substrates were cleaned using ethanol (twice) and 2-propanol (twice) consecutively with sonication and finally rinsed with 2-propanol and dried. These modified substrates were used for multilayer thin film formation using an automatic layer-by-layer (LbL) system. Layer deposition was carried out in the following procedures: (i) amine functionalized substrate was immersed into 17.6 mM 1,3-PDI in 1,4-dioxane and toluene (3:1, v/v) solution for 5 min. Then, the substrate was rinsed in five separate containers: two beakers of 1,4-dioxane and toluene mixture at the previously described ratios, two beakers of dry THF, and finally one beaker of chloroform. (ii) After washing, the isocyanate-terminated substrate was immersed into 3.78 mM TAPM in 1,4-dioxane and toluene (3:1, v/v) solution for 5 min, followed by rinsing successively in two beakers with 3:1 (v/v) ratio of 1, 4-dioxane and toluene mixture, and two beakers of THF. The deposited substrate was dried under Ar atmosphere. This bilayer deposition process described above (steps (i) and (ii)) was designated as a single cycle of molecular layer deposition (MLD). Multilayer thin films were formed by repeating the procedure described above in a desired number of cycles. In every cycle, the amine-terminated surface is regarded as a top surface.

2.3. Characterization

Several analytical techniques have been applied to investigate multilayer growth, to explore the physical and chemical properties of the polyurea thin films, and to elucidate the film surface morphology. UV-vis absorption spectra of the molecular networks fabricated on quartz substrates were obtained using a UV-vis spectrometer (Jasco V-630BIO-IM; Jasco Corp. Japan). The APTMS-modified quartz substrate was used as a background. Fourier-transform infrared (FTIR) spectroscopy was used to investigate the urea bond formation of the thin film on the substrate. Infrared spectra were collected using an FTIR spectrometer (Nicolet 6700; Thermo Fisher Scientific Inc.) equipped with a mercury cadmium telluride (MCT) detector. An APTMS-modified Si wafer was used as a background. Spectra were taken at 8° from the surface normal. The signal noise has been subtracted by smoothing process. To check the surface morphology, an atomic force microscope (AFM, Nanoscope IIIa; Veeco Instruments) with tapping mode was used. Silicon cantilevers (SI-DF3FM; Nanosensors Corp.) with a spring constant between 2.8 Nm^{-1} and 4.4 Nm^{-1} and resonance frequency of 79–89 kHz were used. The measurements were taken, respectively, under an air atmosphere with a scan rate of 0.4 Hz and scan size of 5×5 μm^2 and 0.5×0.5 μm^2. Film thickness was measured using an AFM (VN–8000; Keyence Co.) equipped with a DFM/SS mode cantilever (OP-75041;

Keyence Co.). Thickness was measured at least four positions on each sample and got an average value. Then XPS study was performed using a DLD spectrometer (Kratos Axis-Ultra; Kratos Analytical Ltd.) with an Al Kα radiation source (1486.6 eV). Energy calibration and component separation were conducted using the bundled software with pure Gaussian profiles and a Shirley background. X-ray reflectivity (XRR) analysis was performed using a high-resolution diffractometer (ATX/G; Rigaku Corp.; Japan) with an R-AXIS IV two-dimensional (2D) detector. The diffractometer was equipped with Cu Kα radiation (λ= 0.1542 nm) and divergence of 0.01°. The reflective oscillation curves were fitted using software (GIXRR; Rigaku Corp.; Japan). Curve fitting areas were chosen between 0.3° to 3°. Grazing incidence small angle X-ray scattering (GI-SAXS) analysis was performed using a diffractometer (FR-E; Rigaku Corp., Japan) with beam size of approximately $300 \times 300 \ \mu m^2$. The camera length was 300 mm. The sample stage was composed of the goniometer and a vertical stage (ATS-C316-EM/ALV-300-HM; Chuo Precision Industrial Co. Ltd.). The X-ray incidence angle varied between 0.21° and 0.22°. The X-ray exposure time was fixed for 4 hr.

3. RESULTS AND DISCUSSION

To confirm the multilayer growth of MLD process, transparent UV-vis spectra of thin films were measured as a function of the MLD cycles (Figure 2). The absorption maxima were centered at 268 nm. The absorbance intensities continuously increased within deposition cycles represents the multilayer growth carried out. The inset of Figure 2 shows layer growth near the substrate up to 10 MLD cycles and extending away layer growth above 10 MLD cycles followed two distinctive linear trends. This results suggested non-linear growth for MLD cycles.
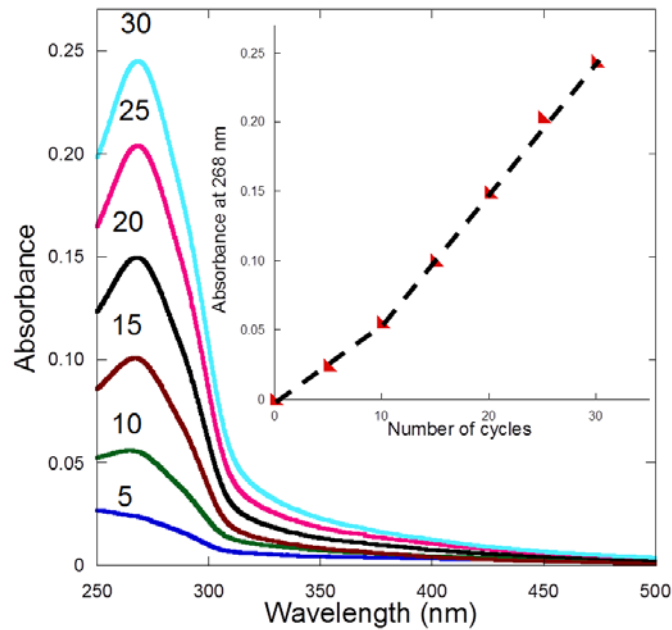

Figure 2. UV-vis spectra of multilayer thin film as the number of deposition cycles on quartz substrate. Inset: absorption peak intensity at 268 nm as a function of 0–30 deposition cycles.

As the absorbance intensity increases (Figure 2) with the number of deposition cycles, thickness also changes with the number of deposition cycles. Film thickness was investigated using AFM and XRR techniques. For AFM thickness measurements, films were partly scratched and the height difference was evaluated for film thickness. Thicknesses of the 10, 20, and 30 MLD cycle films were respectively, 4.34, 6.82, and 9.33 nm thick. These results show growth rates (avg.) of 0.434 nm / cycle, 0.341 nm / cycle and 0.311 nm / cycle, respectively, for 10, 20, and 30 MLD cycle films. The thickness of AFM results is well-matched to the XRR results, as shown in Figure 3. Results of XRR data are discussed later. The non-uniform growth rate (avg.) per cycle in 10, 20, and 30 MLD cycle films might be attributed to different packing conformations (loose/dense) per unit volume (cm^3) of different depth into the films. This density (g/cm^3) change phenomenon will be discussed next. Moreover, this thickness value is lower than the combined molecular length of 1,3-PDI and TAPM, which is estimated as approximately 1.44–1.61 nm / cycle. Some reports of the literature have described that growth rates are much less than ideal repeating unit length for MLD thin film deposition.[1,11,12] This deviation can be explained with several reasons. Thinner growth could be observed because of the tilting of organic molecular networks. In "double" reactions, the bifunctional monomer stops the layer growth by forming a

11

"capped" region on the reactive film surface.[10,11] Finally, steric hindrance due to bulky

precursor may also affect the accessibility of surrounding reactive sites and cause

submonolayer coverage.[1] Though, the growth rate of the polyurea thin film is lower than

expected, the film thickness increased with MLD cycles, indicating multilayer

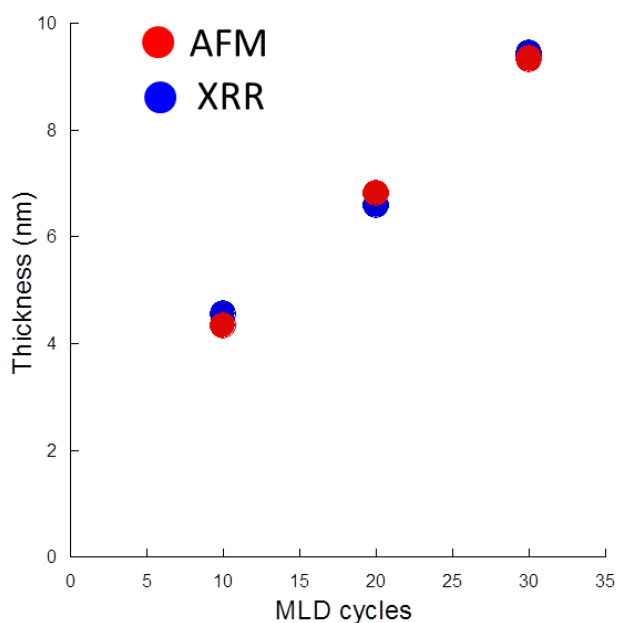deposition. This phenomenon is consistent with the UV-vis results discussed above.

Figure 3. Thickness profiles of 10, 20, and 30 MLD cycle films by AFM (red circle) and

XRR (blue circle).

This increase of UV-vis absorbance intensity and changes of thickness with MLD

cycles does not confirm the formation of a urea bond (covalent networks) into thin films.

Polyurea networks formation through reaction between amine and isocyanate

functionalities was inspected with infrared (IR) spectroscopy. Figure 4 presents IR

spectra of 10, 20, and 30 MLD cycle thin films. Several characteristic peaks were observed in the region of 1200–1800 cm^{-1}. Spectra of the higher wavenumber region are shown in Supporting Information as Figure S2. Peaks around 1650 cm^{-1} – 1690 cm^{-1} can be assigned to the amide I band with the v(C=O) stretching vibration mode of the urea group. The band at 1510 cm^{-1} can be assigned to the amide II band with (N–H) bending vibration. These two bands and the v_a(N-C-N) asymmetric stretching band at 1300 cm^{-1} suggest urea linkage formation. The wavenumbers of these characteristic peaks are consistent with others reported in the literature of polyurea linkage,[26,27,34,35] and assist to confirm polyurea networks in as-synthesized thin films. In addition, a shoulder-type band near 1535 cm^{-1} and a sharp band near 1603 cm^{-1} are respectively attributable to aromatic ring breathing and aromatic ring stretching.
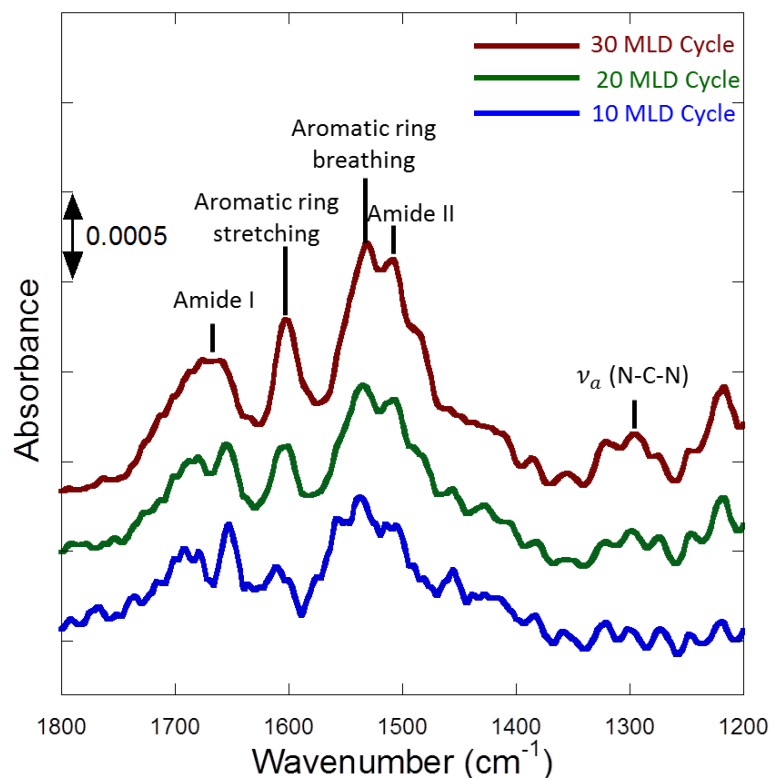
Figure 4. IR spectra of 10, 20, and 30 MLD cycle thin films in the infrared vibrational region for urea bonds. Spectra were measured under a nitrogen atmosphere.

Along with infrared spectroscopy, X-ray photoelectron spectroscopy (XPS) can also be applied to investigate the bonding to as-synthesized polyurea thin films. The atomic environments and chemical bonding to the thin films can be discussed using XPS fine scans spectra. Figure 5 depicts C 1s and N 1s XPS fine scan spectra of 10, 20, and 30 MLD cycle films. Survey scan spectra are shown in Supporting Information (Figure S3).
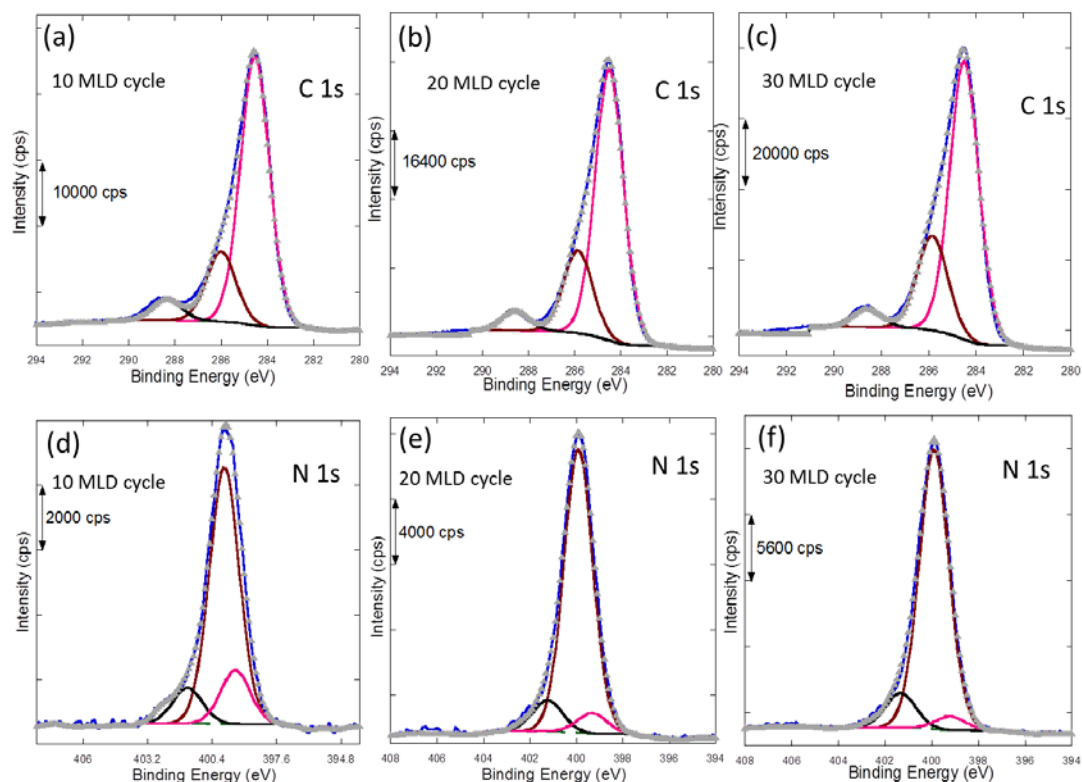
14

Figure 5. XPS fine scan spectra of C 1s (top (a–c)) and N 1s (bottom (d–f)) at 10, 20, and 30 MLD cycle films.

The C 1s fine scan spectra showed three different types of carbon species in all MLD films. The lowest binding energy peak at 284.5 eV resulted from electron rich aromatic carbon. The highest binding energy peak near 288.6 eV resulted from the carbonyl carbon (C=O) from urea linkage. The intermediate peak at 285.9 eV resulted from the combination of alkyl carbon and substituted aromatic carbon linked with urea. These assignments of the C 1s fine scan spectra are consistent with other reports of the polyurea-based and thiourea-based MLD literature.[27,28] These assignments confirm the

urea bond formation into thin films. The IR results also reinforce urea bond formation, indicating that the reaction between amine and isocyanate functionalities form polyurea networks via a urea-coupling reaction.

The N 1s fine scan also contained three isolated peaks. The intermediate binding energy peak at 399.9 eV corresponds to urea groups.[27,33] The lower binding energy at 399.3 eV and higher binding energy at 401.3 eV are attributed respectively to non-hydrogen bonded and hydrogen-bonded free amine groups in polyurea thin films.[36] N 1s for isocyanate was not detected because the unreacted isocyanate groups are converted easily to amine by exposure to humid air.[33]

From Table 1, results show that the peak intensity percentage of N 1s for urea linkage increases from 74% to 85% with layer growth. The urea density apparently increased with layer growth. This revealed that different degrees of cross-linking were formed among layers proximate to the surface and extending away from the surface. This degree of cross-linking might also influence the mass density (g/cm^3) of 10, 20, and 30 MLD cycle films.

Table 1. Peak widths and intensity of the deconvoluted N 1s in 10, 20, and 30 MLD cycle films

	N 1s in urea	N 1s in amine	N 1s in H-bonded amine
10 Cycles			
Binding Energy (eV)	399.9	399.3	401.4
FWHM (eV)	1.49	1.49	1.49
Peak intensity (%)	73.97	15.57	10.44
20 Cycles			
Binding Energy (eV)	399.9	399.3	401.3
FWHM (eV)	1.44	1.49	1.49
Peak intensity (%)	84.0	6.41	9.59
30 Cycles			
Binding Energy (eV)	399.9	399.2	401.3
FWHM (eV)	1.46	1.50	1.49
Peak intensity (%)	84.82	4.30	10.87

However, inspection of the peak intensity ratio of three carbon species is not applicable because of the presence of adventitious carbon (AC) in thin films. This AC carbon might influence the intensity ratio of carbon species. Finally, UV-vis, IR, and XPS results revealed that sequential deposition of amine and isocyanate functionalities produces polyurea networks and demonstrates multilayer growth.

To evaluate the film thickness, film mass density, and interface roughness, XRR measurements were performed. XRR is a powerful tool for accurate measurement of multilayer thin film thickness, film mass density, and interface roughness.[37–39] Figure 6 shows XRR curves for 10, 20, and 30 MLD cycle films. From the XRR simulated fringes of Figure 6, film thickness, film mass density, and roughness of 10, 20, and 30 MLD cycle films were estimated. For XRR fitting curves, the simulated fringe satisfactorily fit with the experimental fringe profile in the case of 10 MLD cycles with a uniform density. In the case of 20 and 30 MLD cycle films, the results of satisfactory fit with a uniform density could not be obtained. More close fit has been tried with a bilayer model as shown in Figure S6. The fit results were found to improve at the sufficiently satisfactory level. The densities around the boundary between the free interface layer and interfacial layer might intergrade. These results suggest the non-uniform density structure in the thicker films. From XRR measurements, the respective thicknesses of 10, 20, and 30 MLD cycle films were found to be 4.55, 6.59, and 9.44 nm thick. This replies nonlinear thickness growth (in average) per cycle with respect to MLD cycles. AFM results support this nonlinear thickness growth as shown in Figure 3. Therefore, it is clear to say that the films density should vary with number of deposition cycles.
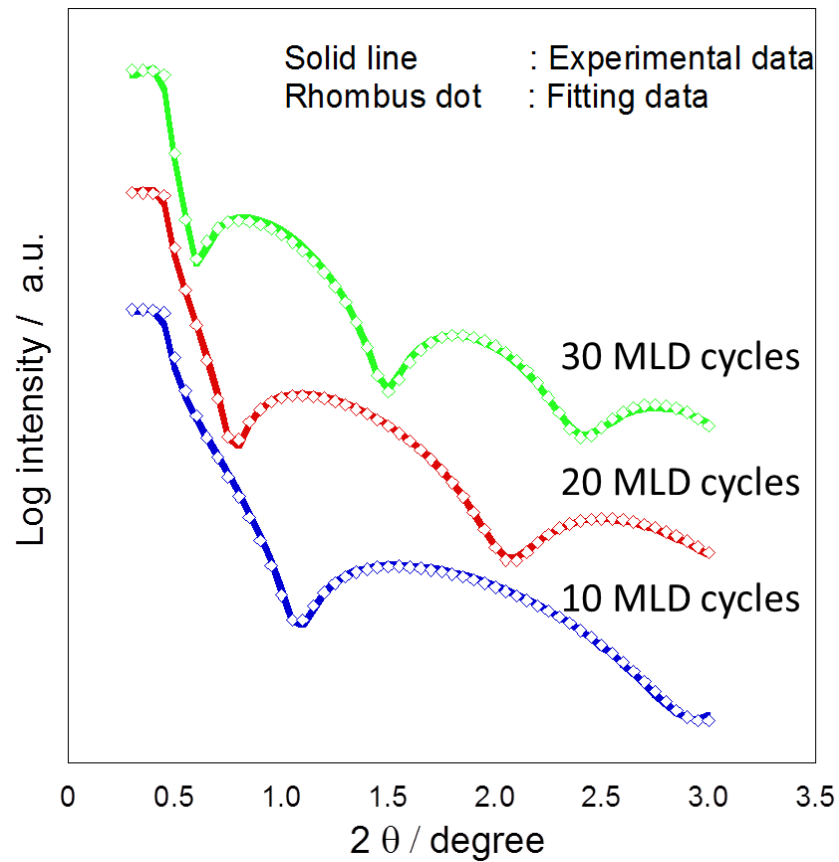
Figure 6. XRR profiles of different MLD cycle thin films. Solid lines and rhombus dot represent experimental and fitting data.

XRR density profiles (Figure 7) showed that the film mass density of 10 MLD cycle film is constant through the film depth. However, for 20 and 30 MLD cycle films, the mass density is not uniform throughout the range of film depths. The mass density of the free interface (f/i) region is ca. 16% higher than that of the interfacial layer (int.) region.
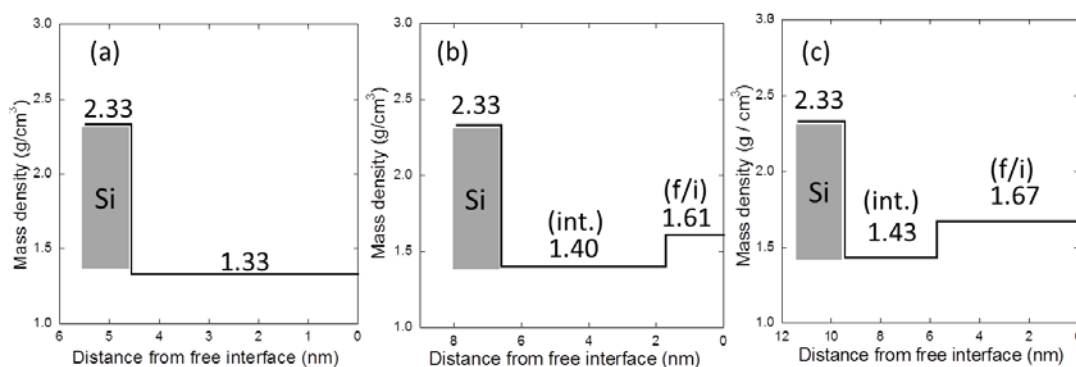
Figure 7. Film mass density (g/cm^3) profiles of simulated models for (a) 10 MLD cycle, (b) 20 MLD cycle, and (c) 30 MLD cycle thin films as a function of distance from the free interface.

These phenomena might occur because of different packing densities proximate to the surface (up to 3.5–5 nm thickness) and extending away from the surface (thicker than 3.5–5 nm). The XPS results support this hypothesis. We assume that these density changes might be observed according to the different degrees of interpenetration among organic molecular networks or different degrees of cross-linking. Since, cross-linking introduces denser film[1] and the XPS results suggest that urea density increases with layer growth. This fact suggests that different degrees of cross-linking occurred among the layers near to the surface and extending away from the surface.

The propensity of cross-linking among molecular networks proximate to the substrate surface and extending away from the substrate surface can be considered with corresponding molecule–molecule interaction. Molecule–molecule interaction in layers

extending away from the substrate surface might be considerably higher than it is near

the substrate surface. Thereby, it is possible to change the degree of cross-linking

proximate to the surface and extending away from the surface. This different degree of

cross-linking can also be examined with changes of molecular volume (Å^3) in single

repeating unit within-layer deposition. Reportedly cross-linking increases the film

density corresponding to the decrease in the molecular volume of each repeating

unit.[1] The repeating unit can be defined by the reactivity of four amine functional groups

as one TAPM molecule with four isocyanate groups as two 1,3-PDI molecules. The

molecular volume of each repeating unit can be extracted approximately by the

mass-to-density ratio using the molecular mass of the single repeating unit and the film

density obtained from XRR density profiles. This analysis revealed that the molecular

volume in the free interface (f/i) region of 20 and 30 MLD cycle films decreases

compared to the interfacial (int.) region (Table 2). The molecular volume of the single

repeating unit in the free interface (f/i) regions of 20 and 30 MLD cycle films are,

respectively, 722 Å^3 and 696 Å^3. In contrast, the molecular volumes of the single

repeating unit in interfacial layers (int.) region of 20 and 30 MLD cycle films are,

respectively, 830 Å^3 and 813 Å^3. This result reflects the presence of different degrees of

cross-linking into thin films. This phenomenon is responsible for introducing nonlinear

mass densities into thin films.

Table 2. Molecular volume of single repeated unit in 10, 20, and 30 MLD cycle films

MLD cycles	Total Thickness (nm)	Thickness (nm)	Mass density (g/cm^3)	Molecular volume (Å^3)
10	4.55	4.55	1.33	874
20	6.59	4.89 (int.)	1.40 (int.)	830 (int.)
		1.70 (f/i)	1.61 (f/i)	722 (f/i)
30	9.44	3.73 (int.)	1.43 (int.)	813 (int.)
		5.71 (f/i)	1.67 (f/i)	696 (f/i)

To increase the film mass density with deposition cycles, structural change might occur. These structural properties of the thin films were evaluated using GI-SAXS. Figure 8 portrays 2D and 1D GI-SAXS profiles of the 30 MLD cycle film on a Si wafer. The GI-SAXS profiles for a 10 MLD cycle film are shown in Supporting Information as Figure S8.
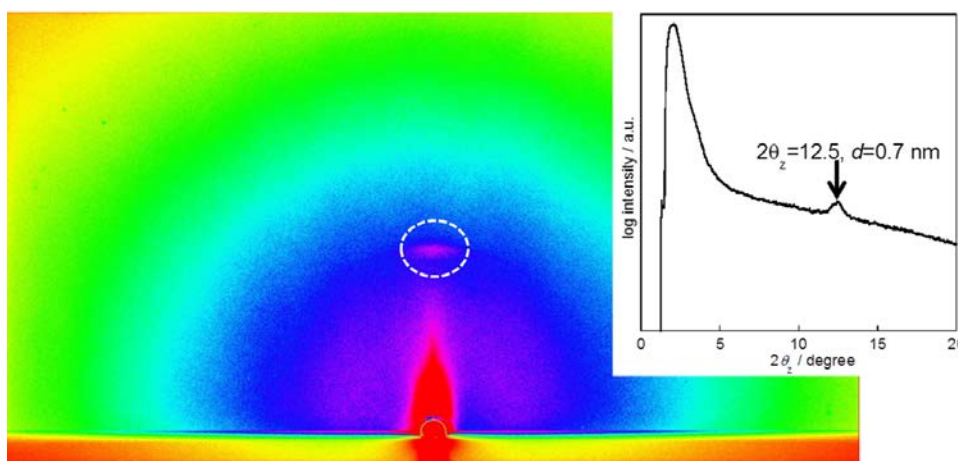

Figure 8. 2D GI-SAXS imaging plate pattern of the 30 MLD cycle film on a Si wafer. 1D profile in the out-of-plane direction extracted from the 2D GI-SAXS pattern.

A clear diffraction was observed in 30 MLD cycle film in 2D imaging plate at the out-of-plane direction at $2\theta_z = 12.5°$ (Figure 8) with a corresponding d-spacing value of 0.7 nm. However, no diffraction peak was observed at the out-of-plane direction in the 10 MLD cycle film. This suggests that the threshold thickness should be considered for molecular ordering of the thin film. This result indicates that molecular ordering seems to be improved to the surface normal direction of the substrate with a certain number of deposited layers. In the in-plane direction, no diffraction peak was observed in 10, 20, or 30 MLD cycle films, which indicates that the MLD thin film exhibits less molecular ordering in the in-plane direction.

4. CONCLUSIONS

Using solution-based MLD technique in ambient conditions, we synthesized 3D covalent bonded organic thin films with variable densities from sequential exposure of bifunctional 1,3-PDI and tetrafunctional TAPM precursors. Our layer-assembled thin films exhibited multilayer growth. Fabricated thin films included three characteristic infrared vibrational bands for urea linkage, confirming polyurea networks' existence in the thin films. Furthermore, in XPS study, peak splitting within N 1s and C 1s corresponded to the values expected for polyurea films. Results showed that structural periodicity and mass density (g/cm^3) of the thin films increased concomitantly with the

number of MLD cycles. These unusual changes might result from different degrees of cross-linking of organic molecular networks proximate to the substrate surface and extending away from the surface. This approach of synthesizing organic molecular networks with higher degrees of cross-linking can be extended to porous substrates that can be used for ion separation membranes.

ASSOCIATED CONTENT

Supporting Information

IR, XPS, AFM, XRR, and GI-SAXS studies of different MLD cycle thin films. This material is available free of charge via the internet at http://pubs.acs.org .

AUTHOR INFORMATION

Corresponding Author

*ynagao@jaist.ac.jp Phone: +81(Japan)-761-51-1541, Fax: +81(Japan)-761-51-1149, Address: 1-1 Asahidai, Nomi, Ishikawa 923-1292, Japan

Notes

The authors declare that they have no competing interest, financial or otherwise, related to this study.

ACKNOWLEDGMENTS

REFERENCES

(1) Zhou, H.; Toney, M. F.; Bent, S. F. Cross-Linked Ultrathin Polyurea Films via Molecular Layer Deposition. *Macromolecules* **2013**, *46*, 5638-5643.

(2) Richert, L.; Engler, A. J.; Discher, D. E.; Picart, C. Elasticity of Native and Cross-Linked Polyelectrolyte Multilayer Films. *Biomacromolecules* **2004**, *5*, 1908-1916.

(3) Such, G. K.; Quinn, J. F.; Quinn, A.; Tjipto, E.; Caruso, F. Assembly of Ultrathin Polymer Multilayer Film by Click Chemistry. *J. Am. Chem. Soc.* **2006**, *128*, 9318-9319.

(4) Quinn, J. F.; Johnston, A. P. R.; Such, G. K.; Zelikin, A. N.; Caruso, F. Next

Generation, Sequentially Assembled Ultrathin Films: Beyond Electrostatics. *Chem. Soc. Rev.* **2007**, *36*, 707-718.

(5) Wang, C.; Lee, W-Y.; Nakajima, R.; Mei, J.; Kim, D. H.; Bao, Z. Thiol–Ene Cross-Linked Polymer Gate Dielectrics for Low-Voltage Organic Thin-Film Transistor. *Chem. Mater.* **2013**, *25*, 4806-4812.

(6) Wang, Y; Kim, Y.; Lee, E; Kim, H. Fabrication of Organic Thin-Film Transistors Based on Cross-Linked Hybrid Dielectric Materials. *Jpn. J. Appl. Phys.* **2012**, *51*, 09MJ02 (1-5).

(7) Geise, G. M.; Lee, H. S.; Miller, D. J.; Freeman, B. D.; Mcgrath, J. E.; Paul, D. R. Water Purification by Membranes: The Role of Polymer Science. *J. Polym. Sci. Part B: Polym. Phys.* **2010**, *48*, 1685-1718.

(8) Yimsiri, P.; Mackley, M. R. Spin and Dip Coating of Light Emitting Polymer Solution: Matching Experiment with Modeling. *Chem. Eng. Sci*. **2006**, *61*, 3496-3505.

(9) Ulman, A. *An Introduction to Ultrathin Organic Films from Langmuir–Blodgett to Self-Assembly*; Academic Press: San Diego, CA, 1991.

(10) George, S. M.; Yoon, B.; Dameron, A. A. Surface Chemistry for Molecular Layer Deposition of Organic and Hybrid Organic-Inorganic polymers. *Acc. Chem. Res.*

2009, *42*, 498-508.

(11) Zhou, H.; Bent, S. F. Fabrication of Organic Interfacial Layers by Molecular Layer

Deposition: Present Status and Future Opportunities. *J. Vac. Sci. Technol., A* **2013**,

31, 040801-040818.

(12) Sundberg, P.; Karppine, M. Inorganic–Organic Thin Film Structures by Molecular

Layer Deposition: A review. *Beilstein J. Nanotechnol.* **2014**, *5*, 1104-1136.

(13) Seo, J.; Schattling, P.; Lang, T.; Jochum, F.; Nilles, K.; Theato, P.; Char, K.

Covalently Bonded Layer-by-Layer Assembly of Multifunctional Thin Films

Based on Activated Esters. *Langmuir* **2010**, *26*, 1830-1836.

(14) Guin, T.; Cho, J. H.; Xiang, F.; Ellison, C. J.; Grunlan, J. C. Water-Based Melanin

Multilayer Thin Films with Broadband UV Absorption. *ACS Macro Lett.* **2015**, *4*,

335-338.

(15) Adamczyk, N. M.; Dameron, A. A.; George, S. M. Molecular Layer Deposition of

Poly(p-phenyleneterephthalamide) Films Using Terephthaloyl Chloride and

p-Phenylenediamine. *Langmuir* **2008**, *24*, 2081-2089.

(16) Du, Y.; George, S. M. Molecular Layer Deposition of Nylon 66 Films Examined

Using in situ FTIR Spectroscopy. *J. Phys. Chem. C* **2007**, *111*, 8509-8517.

(17) Peng, Q.; Efimenko, K.; Genzer, J.; Pardsons, G. N. Oligomer Orientation in

Vapor-Molecular-Layer-Deposited Alkyl-Aromatic Polyamide films. *Langmuir* **2012**, *28*, 10464-10470.

(18) Bizer, T.; Richardson, N. V. Demonstration of an Imide Coupling Reaction on a Si(100) -2 ✕1 Surface by Molecular Layer Deposition. *Appl. Phys. Lett.* **1997**, *38*, 268-270.

(19) Yoshimura, T.; Tatsuura, S.; Sotoyama, W. Polymer Films Formed with Monolayer Growth Steps by Molecular Layer Deposition. *Appl. Phys. Lett.* **1991**, *59*, 482-484.

(20) Yoshida, S.; Ono, T.; Esashi, M. Deposition of Conductivity-Switching Polyimide Film by Molecular Layer Deposition and Electrical Modification using Scanning Probe Microscope. *Micro. Nano Lett.* **2010**, *5*, 321-323.

(21) Yoshida, S.; Ono, T.; Esashi, M. Local Electrical Modification of a Conductivity-Switching Polyimide Film Formed by Molecular Layer Deposition. *Nanotechnology* **2011**, *22*, 335302.

(22) Haq, S.; Richardson N. V. Organic Beam Epitaxy Using Controlled PMDA−ODA Coupling Reactions on Cu{110}. *J. Phys. Chem. B* **1999**, *71*, 5256-5265.

(23) Lee, J. S.; Lee, Y. J.; Tae, E. L.; Park, Y. S.; Yoon, K. B. Synthesis of Zeolite as ordered Multicrystal Arrays. *Science* **2003**, *301*, 818-821.

(24) Prasittichai, C.; Zhou, H.; Bent, S. F. Area Selective Molecular Layer Deposition of

Polyurea Films. *ACS Appl. Mater. Interfaces* **2013**, *5*, 13391-13396.

(25) Zhou, H.; Bent. S. F. Molecular Layer Deposition of Functional Thin Films for Advanced Lithographic Patterning. *ACS Appl. Mater. Interfaces* **2011**, *3*, 505-511.

(26) Kim, A.; Filler, M. A.; Kim, S.; Bent, S. F. Layer-by-Layer Growth on Ge (100) via Spontaneous Urea Coupling Reactions. *J. Am. Chem. Soc.* **2005**, *127*, 6123-6132.

(27) Loscutoff, P. W.; Zhou, H.; Clendenning, S. B.; Bent, S. F. Formation of Organic Nanoscale Laminates and Blends by Molecular Layer Deposition. *ACS Nano* **2010**, *4*, 331-341.

(28) Loscutoff, P. W.; Lee, H. B. R.; Bent S. F. Deposition of Ultrathin Polythiourea Films by Molecular Layer Deposition. *Chem. Mater*. **2010**, *22*, 5563-5569.

(29) Ivanova, Y. V.; Maydannik, P. S.; Cameron, D. C. Molecular Layer Deposition of Polyethylene Terephthalate Thin Film. *J. Vac. Sci. Technol., A* **2012**, *30*, 01A121 (1-5).

(30) Qian, H.; Li, S.; Zheng, J.; Zhang, S. Ultrathin Films of Organic Networks as Nanofiltration Membranes via Solution-Based Molecular Layer Deposition. *Langmuir* **2012**, *28*, 17803-17810.

(31) Johnson, P. M.; Yoon, J.; Kelly, J. Y.; Howarter, J. A.; Stafford, C. M. Molecular Layer-by-Layer Deposition of Highly Crosslinked Polyamide Films. *J. Polym. Sci.*

Part B: Polym. Phys. **2012**, *50*, 168-173.

(32) Chan, E. P.; Lee, J-H.; Chung, J. Y.; Stafford, C. M. An Automatic Spin-Assisted

Approach for Molecular Layer-by-Layer Assembly of Crosslinked Polymer Thin

Films. *Rev. Sci. Instrum.* **2012**, *83*, 114102 (1-6).

(33) Kim, M.; Byeon, M.; Bae, J-S.; Moon, S. Y.; Yu, G.; Shin. K.; Basarir, F.; Yoon, T.

H.; Park, J-W. Preparation of Ultrathin Films of Molecular Networks through

Layer-by-Layer Cross-Linking Polymerization of Tetrafunctional Monomers.

Macromolecules **2011**, *44*, 7092-7095.

(34) Kohli, P.; Blanchard, G. J. Applying Polymer Chemistry to Interfaces:

Layer-by-Layer and Spontaneous Growth of Covalently Bound Multilayers.

Langmuir **2000**, *16*, 4655-4661.

(35) Coleman, M. M.; Sobkowiak, M.; Pehlert, G. J.; Painter, P. C.; Iqbal, T. Infrared

Temperature Studies of a Simple Polyurea. *Macromol. Chem. Phys.* **1997**, *198*,

117-136.

(36) Graf, N.; Yegen, E.; Gross, T.; Lippitz, A.; Weigel, W.; Krakert, S.; Terfort, A.;

Unger, W. E. S. XPS and NEXAFS Studies of Aliphatic and Aromatic Amine

Species on Functionalized Surfaces. *Surf. Sci.* **2009**, *603*, 2849-2860.

(37) Haque, H. A.; Hara, M.; Nagano, S.; Seki, T. Photoinduced In-Plane Motions of

Azobenzene Mesogens Affected by the Flexibility of Underlying Amorphous Chains. *Macromolecules* **2013**, *46*, 8275-8283.

(38) Chason, E.; Mayer, T. M. Thin Film and Surface Characterization by Specular X-ray Reflectivity. *Critical Rev. Solid State Mat. Sci.* **1997**, *22*, 1-67.

(39) Stove, K.; Sakurai, K. Recent Theoretical Models in Grazing Incidence X-ray Reflectometry. *The Rigaku J.* **1997**, *14*, 22-37.

Table of Contents (TOC)